JCTC Journal of Chemical Theory and Computation

Theoretical and Crystallographic Study of the Dual σ/π Anion Binding Affinity of Quinolizinylium Cation

Carolina Estarellas, Antonio Frontera,* David Quiñonero, and Pere M. Deyà*

Departament de Química, Universitat de les Illes Balears, 07122 Palma de Mallorca, Spain

Received August 12, 2008

Abstract: Benzoquinolizinylium salts are important compounds in the regulation of transmembrane conductance regulator channels. In this manuscript, the geometrical position (σ/π) of the counteranion in quinolizinylium salts has been studied by means of ab initio calculations at the RI-MP2(full)/6−31++G** level of theory. A search in the Cambridge Structural Database determines that the position of the anion depends upon its nature. Halogen anions prefer anion−σ interactions, and BF_4^- and PF_6^- anions prefer anion−π interactions. The dual σ/π binding affinity of title compound has been studied by means of ab initio and molecular interaction potential with polarization (MIPp) calculations and the Bader's theory of "atoms-in-molecules".

I. Introduction

Noncovalent interactions play a decisive role in many areas of modern chemistry. This is especially true in the field of supramolecular chemistry and molecular recognition.[1] Interactions involving aromatic rings are important binding forces in both chemical and biological systems, and they have been reviewed by Meyer et al.[2]

At the same time, Mascal et al.,[3] Alkorta et al.,[4] and our group[5] have demonstrated, theoretically, that the π-interaction of anions with electron deficient aromatic rings is favorable. A pioneering manuscript describing gas-phase clustering reactions between anions and hexafluorobenzene using both theoretical and experimental results was previously reported.[6] Our group has used the term "anion−π interaction"[7] to describe the interaction between anions and hexafluorobenzene, where the anion is positioned over the ring along the C_6 axis.[5] The anion−π interaction is dominated by electrostatic and anion-induced polarization terms.[4,5] The strength of the electrostatic component depends upon the value of Q_{zz}, and the anion induced polarization term correlates with the molecular polarizability ($\alpha_{||}$) of the aromatic compound.[8] Anion−π complexes have been observed experimentally, sustaining the theoretical predictions and the promising proposal for the use of anion receptors based on anion−π interactions in molecular recognition.[9−13] These interactions

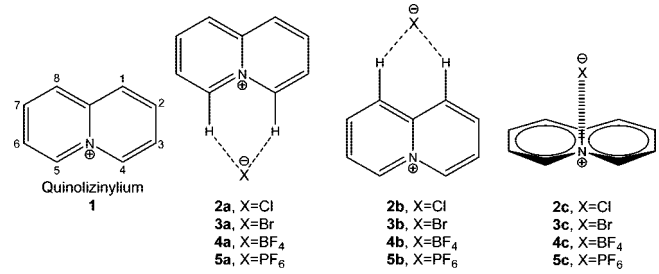

Figure 1. Quinolizinylium cation **1** and its anion−π/σ complexes **2**−**5**.

are also important in ADN bases, such as adenine.[14] Moreover, Berryman et al. have reported structural criteria for the design of anion receptors based on the interaction of halides with electron-deficient arenes.[15] Recent excellent reviews deal with anion-binding involving π-acidic heteroaromatic rings.[16]

Chloride channels play important roles in homeostasis and regulate cell volume, transepithelial transport, and electrical excitability.[17] The cystic fibrosis transmembrane conductance regulator (CFTR) is a cAMP-regulated epithelial chloride channel, mutations in which cause cystic fibrosis.[18] This syndrome is the most common lethal autosomal recessive genetic disease in caucasians. It has been demonstrated that benzoquinolizinylium chloride salts activate both wild-type and mutant cystic fibrosis transmembrane conductance regulator channels.[19] In this manuscript, we report a computational study, where we analyze the geometrical and

* To whom correspondence should be addressed. E-mail: toni.frontera@uib.es.

10.1021/ct800332y CCC: $40.75
Published on Web 10/10/2008

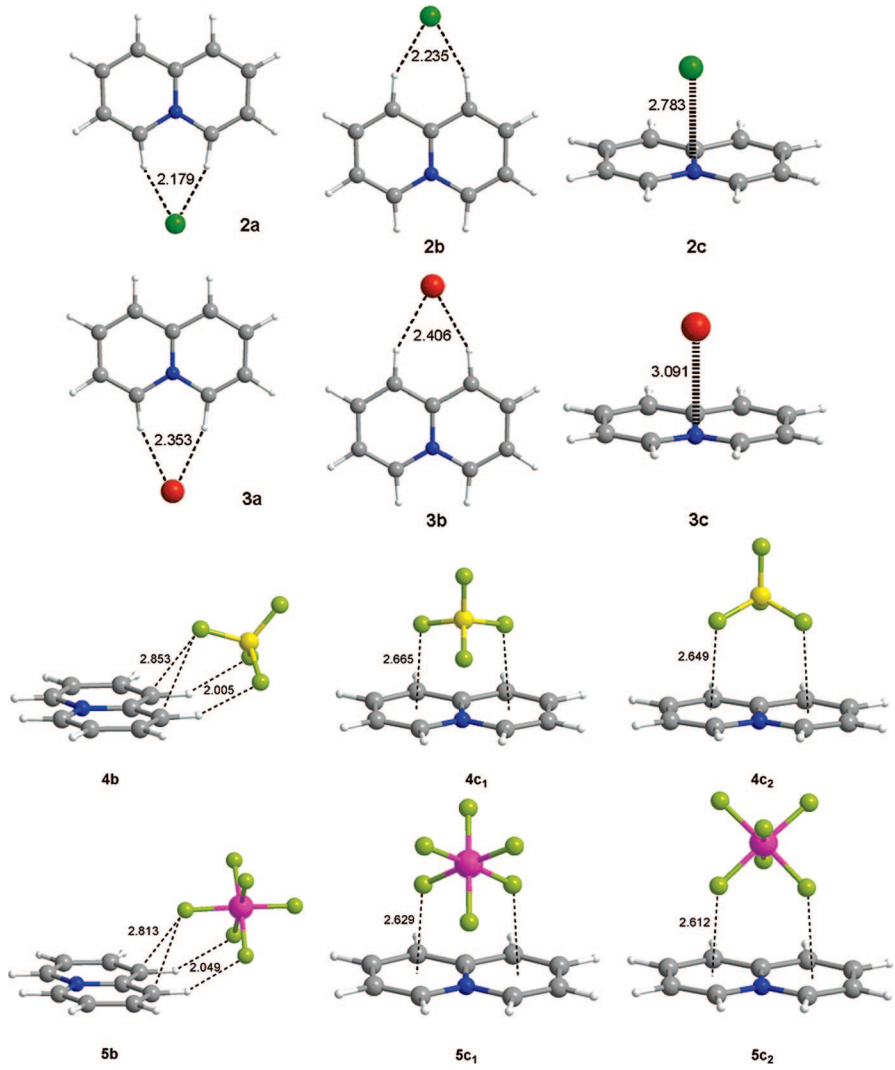

Figure 2. RI-MP2/6−31++G** optimized complexes **2**−**5**. Distances in Å.

energetic features of anion−π and anion−σ complexes of several anions with quinolizinylium cation **1**, also known as quinolizinium. It has been recently reported a combined experimental and theoretical study that deals with the structural criteria for the design of anion receptors based on electron-deficient arenes.[15] The presence of electron-withdrawing groups (EWG) increases the acidity of the arene C−H donors, and consequently, it has a double effect. First, the anion can interact via hydrogen bonding with the arene because the presence of EWG strengthens the C−H···X$^-$ interaction. Second, the anion can also interact with the π-cloud of the arene because the presence of EWG increases the π-acidity of the ring. Cationic aromatic rings can be considered as an extreme of this situation. The aromatic ring is obviously electron-deficient because of its cationic character. In addition, all hydrogen atoms of the ring are available for hydrogen bonding because they have not been substituted by EWGs and their acidity is increased with respect to neutral aromatic rings. Recently, Alkorta el al. have studied a related system, the case of pentazolo[1,2-*a*]pentazole, (N_8) with neutral electron donors, hydrogen-bond donors, and anions.[20] The quinolizinylium cation can interact with the counterion either via the C−H aromatic groups (σ interaction, i.e., hydrogen-bonded complex) or via an anion−π interaction. This dual σ/π binding affinity of **1** has been studied by means of ab initio and molecular interaction potential with polarization (MIPp) calculations, and the Bader's theory of "atoms-in-molecules".

Energetically, in relation to the cation−π interaction, the anion−π interaction is less favorable because the van der Waals radii of anions are bigger than cations, and consequently, the equilibrium distances are larger in anion−π complexes than in cation−π complexes.[21]The energetic terms that contribute to the stabilization of ion−π interactions (electrostatic and polarization) are very dependent on the distance. Therefore, the potential use of electron-deficient aromatic rings as building blocks for the construction of anion receptors[22] is handicapped with respect to the widely use of cation receptors based on cation−π interactions. Inspired by guanidinium salts that combine both hydrogen bonding and electrostatic forces to bind anions, we have recently proposed that a possible solution to solve this disadvantage is the use of charged aromatic compounds that increment the anion-binding ability of the ring.[23] The quinolizinylium cation is an example. Exploring the Cambridge Structural Database (CSD), we have found compounds containing quinolizinylium exhibiting anion−π/σ interactions in the solid state. These interactions have an active influence

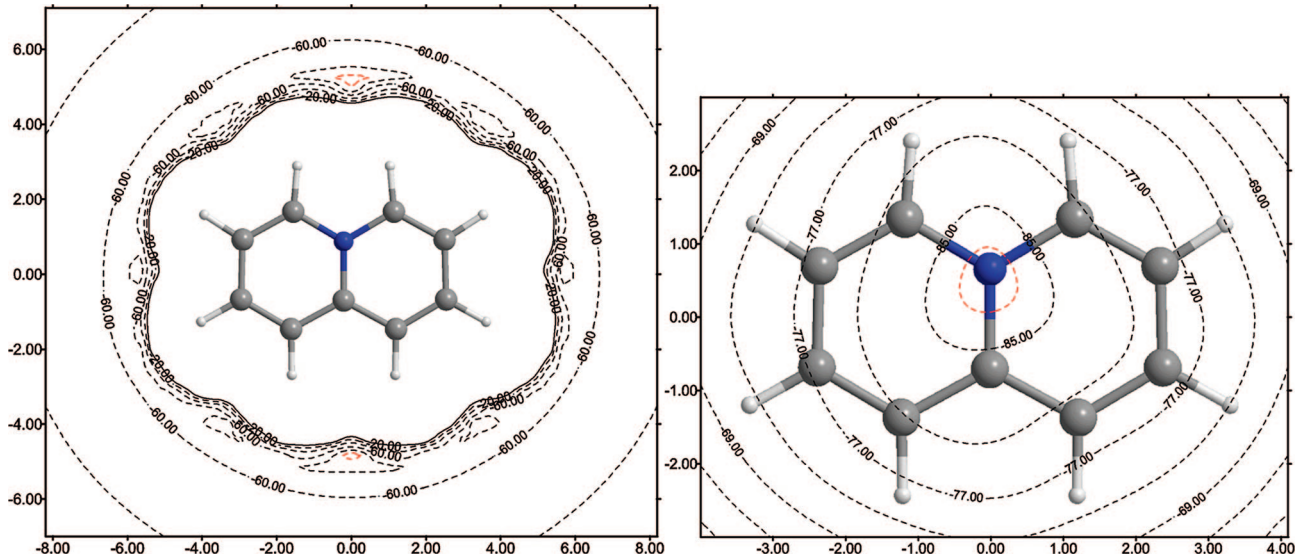

Figure 3. Right: 2D-MIPp(Cl^-) energy map computed for **1** at 2.8 Å above the molecular plane. Isocontour lines are plotted every 4 kcal/mol. The lowest energy isocontour is ploted in red. Axes units are Å, and energies are in kcal/mol. Left: 2D-MIPp(Cl^-) energy maps computed for **1** at the molecular plane. Isocontour lines are plotted every 10 kcal/mol. The lowest energy isocontour is plotted in red.

Table 1. Interaction Energies at the RI-MP2(full)/6-31++G** Level of Theory without and with the BSSE Corrections (E and E_{BSSE}, kcal/mol) and Equilibrium Distances (R_e, Å)[a]

compound	NImag	E	E_{BSSE}	R_e	q (e) M-K	q (e) Mull
2a	0	−92.02	−86.23	2.179[b]	−0.82	−0.72
2b	0	−85.94	−80.35	2.235[b]	−0.83	−0.73
2c	0	−89.42	−81.56	2.783[c]	−0.77	−0.70
3a	0	−87.88	−82.80	2.353[b]	−0.79	−0.81
3b	0	−82.43	−77.38	2.406[b]	−0.82	−0.78
3c	0	−87.58	−81.60	3.091[c]	−0.81	−0.72
4a	Stationary point not found, it converges to **4c**					
4b	0	−78.27	−74.26	2.005[d]	−0.85	−0.87
$4c_1$	0	−86.38	−79.30	3.220[e]	−0.78	−0.89
$4c_2$	0	−84.64	−77.80	3.195[e]	−0.77	−0.91
5a	Stationary point not found, it converges to **5c**					
5b	0	−73.88	−68.98	2.049[d]	−0.86	−0.89
$5c_1$	0	−82.57	−74.31	3.662[e]	−0.80	−0.92
$5c_2$	0	−81.04	−72.98	3.639[e]	−0.79	−0.92

[a] The computed Merz−Kollman (M-K) and Mulliken (Mull) charges of the anion (q, e) are also included for both hydrogen-bonded and π-complexes. [b] R_e is the mean distance of two C−H···X^- distances. [c] R_e is measured from the anion to the middle of the bridge C−N bond. [d] Measured from the F atom to the H atom of the ring as shown in Figure 2. [e] Measured from the B/P atom to the middle of the common C−N bond.

in the crystal packing of the quinolizinylium cation and the location of the anion agrees with the theoretical calculations.

II. Theoretical Methods

The geometry of all the complexes included in this study was fully optimized at the RI-MP2/6−31++G** level of theory within the program TURBOMOLE, version 5.7.[24] The RI-MP2 method[25,26] applied to the study of cation−π and anion−π interactions is considerably faster than the MP2 and the interaction energies, and equilibrium distances are almost identical for both methods.[27,28] The binding energy was calculated at the same level with and without correction for the basis set superposition error (BSSE) using the Boys−Bernardi counterpoise technique.[29] No symmetry constraints have been imposed in the optimizations, and all compounds and complexes belong to the C_1 symmetry point group. Frequency calculations at the same level of theory have confirmed the minimum nature of all complexes.

The contributions to the total interaction energy have been computed using the molecular interaction potential with polarization (MIPp) methodology,[30] which is an improved generalization of the molecular electrostatic potential (MEP), where three terms contribute to the interaction energy: (i) an electrostatic term identical to the MEP,[31] (ii) a classical dispersion−repulsion term, and (iii) a polarization term derived from perturbation theory.[32] Calculation of the MIPp of **1** with F^- and Cl^- anions was performed using the HF/6−31++G**//RI-MP2(full)/6−31++G** wave function of the aromatic rings by means of the MOPETE-98 program.[33] Calculation of MIPp using the MP2 wave function are not available.[33] The ionic van der Waals parameters for F^- and Cl^- were taken from the literature.[34]

The topological analysis of the electron charge density performed for the complexes of **1** with anions was determined using Bader's theory of "atoms-in-molecules" (AIM).[35] The electronic density analysis was performed using the AIM2000 program[36] at the MP2//RI-MP2 level of theory. We have evaluated the charge transfer in the complexes by using the Merz−Kollman (M-K) scheme for deriving atomic charges at the MP2/6−31++G**//RI-MP2(full)/6−31++G** level of theory. It has been reported that this method provides high quality charges.[37] The Mulliken charges[38] are also included for comparison purposes.

III. Results and Discussion

A. Energetic and Geometrical Details. Table 1 reports the energies and equilibrium distances corresponding to the interaction of **1** with several anions via either hydrogen bonding (**2a**−**5a** and **2b**−**5b**) or anion−π (**2c**−**5c**) binding

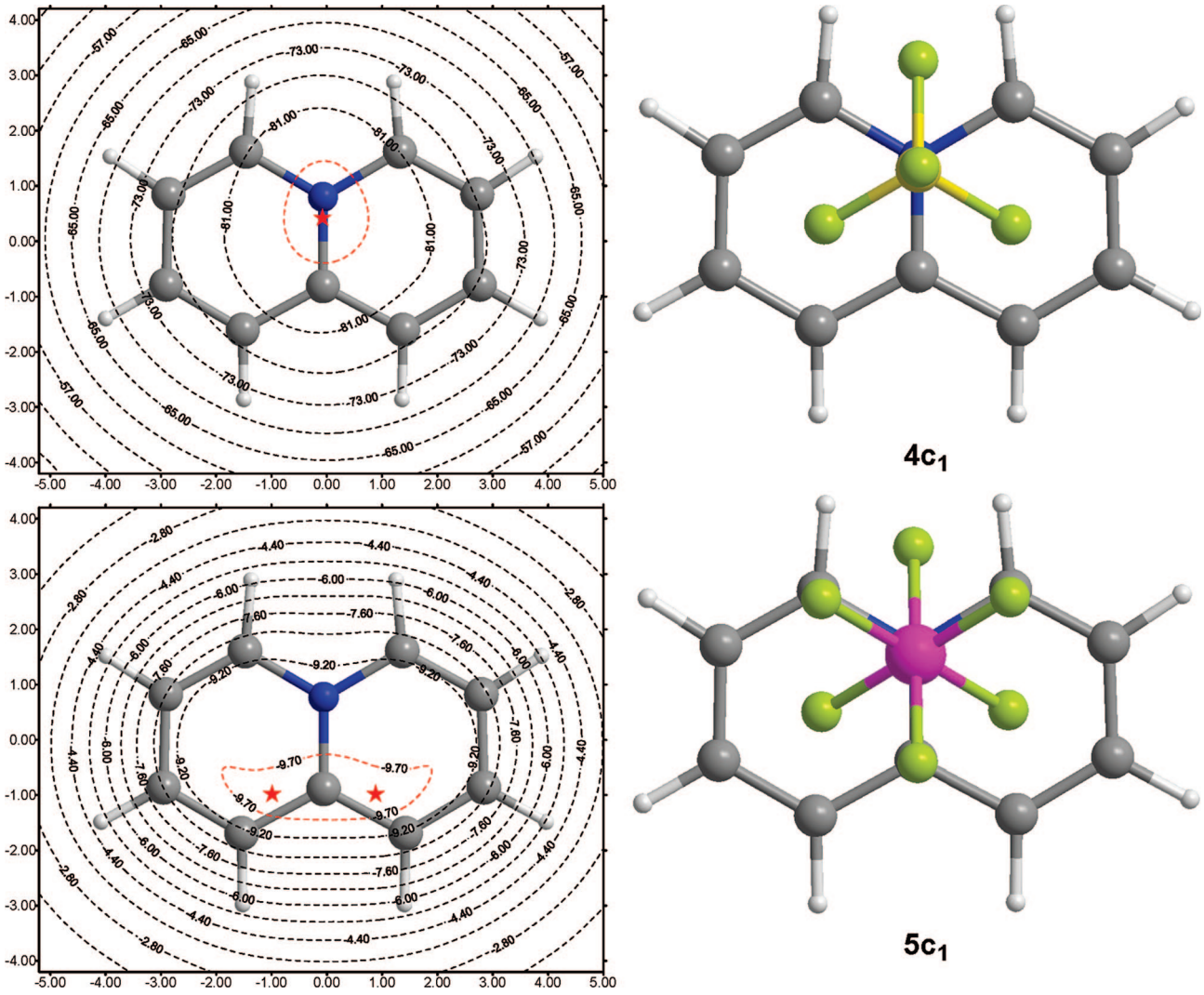

Figure 4. Right: Zenithal views of the optimized anion−π complexes **4c$_1$** and **5c$_2$**. Left, bottom: 2D-IPE(F^-) energy map computed for **1** at 2.8 Å above the molecular plane. Isocontour lines are plotted every 0.8 kcal/mol. Left, top: 2D-MIPp(F^-) energy map computed for **1** at 2.8 Å above the molecular plane. Isocontour lines are plotted every 4 kcal/mol. In both maps, the lowest-energy isocontour is plotted in red. Axes units are Å, and energies are in kcal/mol. The global minima are represented by red stars.

types. The geometry of the optimized complexes is depicted in Figure 2. For all complexes, the interaction energies are large and negative because of the ion−pair nature of the interaction. From the inspection of the results, several interesting points arise. First, the most favorable situation for the complexation of **1** with Cl^- and Br^- is the hydrogen bonding interaction via the hydrogen atoms that are in α with respect to the aromatic nitrogen atom (**2a** and **3a**). Moreover, the anion−π complexes **2c** and **3c** are more favorable than the hydrogen bonding complexes **2b** and **3b**, indicating that the π-binding mode is more favorable than the σ-interaction (bifurcated hydrogen bond) with both H^1 and H^8 hydrogen atoms (see Figure 1 for the numbering of **1**). A differentiating feature between anion-π complexes **2c** and **3c** is that the chloride anion lies approximately over the carbon atom of the C−N common bond whereas the bromide anion lies approximately over the nitrogen atom of the common bond. We have explored all possible binding modes between **1** and the Cl^- anion through hydrogen bonding interactions, and in all cases, they converge to either **2a** or **2b**. The same result was obtained in the bromide complexes. Second, a different behavior is observed in the complexes of poliatomic anions BF_4^- and PF_6^-. For both anions, the hydrogen bonding complexes **4a** and **5a** are not found; they converge to the anion−π complexes **4c** and **5c**, respectively. This indicates that both anions prefer the π-binding mode with **1**. Moreover, for both anions, the π-complexes are considerably more favorable energetically than the hydrogen bonding complexes (**4b** and **5b**). For the anion−π complexes **4c** and **5c**, two favorable orientations for the anion have been found, namely, **4c$_1$**, **4c$_2$**, **5c$_1$** and **5c$_2$**, see Figure 2 for details. Complexes **4c$_1$** and **5c$_1$** are slightly more favorable than **4c$_2$** and **5c$_2$**, respectively. Third, in Table 1, we also include the charge of the anion in the complexes to study charge transfer effects. We have used two methods for deriving the atomic charges, Mulliken and Merz−Kollman (M-K). It has been demonstrated that the latter method provides high-quality charges. It can be observed that in all complexes, the charge transfer (M-K) is important (about 0.2 e). Moreover, charge transfer is less important in hydrogen bonding complexes

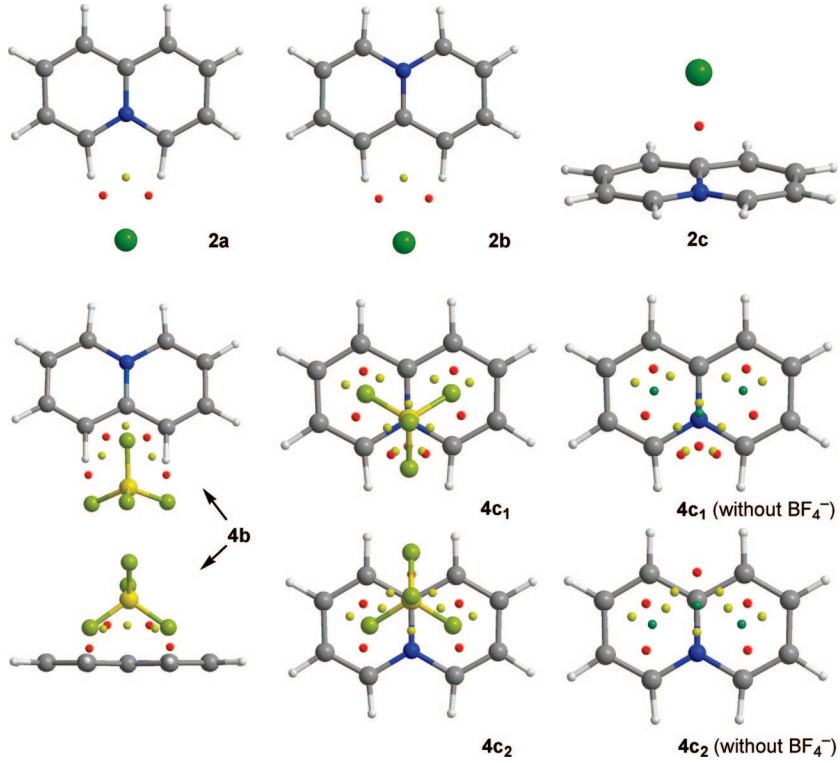

Figure 5. Schematic representation of the critical points that emerge upon complexation of the anion for complexes **2a**−**2c** and **4b**−**4c**. Bond CPs are represented in red; ring CPs are in yellow, and cage CPs are in green.

Table 2. Electron Density (ρ) and Its Laplacian ($\nabla^2\rho$) in Atomic Units at the Critical Points (CP) Originated upon Complexation and the Number (n) of each CP in the complex, Computed at the MP2/6-31++G**//RI-MP2/6-31++G** Level of Theory[a]

compound	n	CP	$10^2\rho$	$10\nabla^2\rho$
2a	2	(3, −1)	2.780	0.706
	1	(3, +1)	1.207	0.581
2b	2	(3, −1)	2.473	0.662
	1	(3, +1)	0.906	0.459
2c	1	(3, −1)	2.594	0.704
3a	2	(3, −1)	2.369	0.564
	1	(3, +1)	1.107	0.494
3b	2	(3, −1)	2.212	0.535
	1	(3, +1)	0.833	0.392
3c	1	(3, −1)	1.602	0.522
4b	2	(3, −1)	2.057	0.733
4c$_1$	1	(3, +3)	0.622	0.379
4c$_2$	1	(3, +3)	0.568	0.362
5b	2	(3, −1)	1.835	0.677
5c$_1$	1	(3, +3)	0.561	0.397
5c$_2$	1	(3, +3)	0.515	0.342

[a] For complexes **4b** and **5b**, only the CPs that describe the σ-interaction are summarized. For complexes **4c** and **5c**, only the cage CPs that describe the interaction of the B/P with **1** are summarized.

than in π-complexes, apart from bromide complexes, probably because of the larger equilibrium distance of the anion−π complex **3c** (3.091 Å). Mulliken charges do not follow the same trend. In some cases, they indicate a large charge transfer (0.3 e in **2c**), and in other cases, they indicate a very small charge transfer (0.08 e in **5c**). These inconsistencies confirm the low quality of the charges obtained from the Mulliken population analysis, in agreement with previous observations.[37]

The geometric features of complexes **2**−**5** are shown in Figure 2. The equilibrium distances of complexes **2a** and **3a** are shorter than the ones computed for **2b** and **3b**, respectively, in agreement with the energetic results. In the hydrogen-bonded complexes **2a**-**2b** and **3a**-**b**, the anion interacts simultaneously with two hydrogen atoms. Experimentally, it has been demonstrated that bifurcated hydrogen bonds to two neighboring CH groups are energetically favored over linear hydrogen bonds to a single CH groups.[39] The hydrogen bonding complexes **4b** and **5b** present a peculiar geometry, see Figure 2, where the anion is not coplanar with the quinolizinylium rings. Two fluorine atoms of the anion interact with two hydrogen atoms (H^1 and H^8), and another fluorine atom interacts with two carbon atoms of the ring (C^1 and C^8). Finally, in the anion−π complexes, **4c$_{1-2}$** and **5c$_{1-2}$**, the anion is located approximately over the center of the bridge C−N bond. Two fluorine atoms point to the ring centroids and a third fluorine atom is located approximately over the nitrogen atom in **4c$_1$** and **5c$_1$** and over the carbon atom of the common bond in **4c$_2$** and **5c$_2$**.

B. MIPp Analysis. With the purpose of analyzing the nature of the anion−π/σ interaction in the quinolizinylium cation and understanding the importance of electrostatic and polarization terms, we have performed the calculation of MIPp of **1** interacting with F^- and Cl^- using the HF/6−31++G**//RI-MP2(full)/6−31++G** wave function. In the calculations, the F^- and Cl^- ions were considered as a classical nonpolarizable particles. In Figure 3, we represent the bidimensional MIPp (2D-MIPp) maps obtained for **1** interacting with Cl^-. We have computed two 2D-MIPp maps, one at the molecular plane and the other at 3.0 Å over the molecular plane and parallel to it to study the anion-binding

Table 3. Reference Codes of the X-ray Structures That Include the Quinolizinylium Moiety, the Counterion, the Type of Interaction and References

CSD reference	entry	anion	interaction	ref
AZPHNE	1	Cl^-	σ	47
CIPQOH	2	Br^-	σ	48
CIPQUN	3	Br^-	σ	48
CIPROI	4	BF_4^-	σ and π	48
DANJAD	5	Br^-	σ	49
DAVPOG	6	BF_4^-	σ and π	50
DAVPUM	7	BF_4^-	σ and π	50
GUKTEL	8	PF_6^-	σ	51
IDIFAD	9	BF_4^-	σ and π	52
IXUJEQ	10	Cl^-	σ	19
IXUJIU	11	Cl^-	σ	19
IXUJOA	12	Br^-	σ	19
KASVOP10	13	PF_6^-	σ and π	45
KIHGOX	14	BF_4^-	σ and π	46
LUCGEV	15	Br^-	σ	53
LUCGIZ	16	Br^-	σ	53
TATZOE	17	$CH_3SO_3^-$	σ and π	54
TATZUK	18	Cl^-	σ	54
TAVBIC	19	$CH_3SO_3^-$	σ and π	54
TAVBOI	20	Cl^-	σ	54
ULATIK	21	Cl^-	σ	55
WEPTEQ	22	Br^-	σ	56
WUXKAB	23	PF_6^-	σ and π	57

ability of **1**, first via hydrogen bonding using the hydrogen atoms of the ring and second via an anion-π interaction, respectively. It can be observed a good agreement between the location of the minima in the 2D-MIPp energy maps and the geometry of the optimized complexes. For instance, it can be observed that in the 2D-MIPp(Cl^-) energy map computed at the molecular plane several local minima are observed, each of them corresponds to the interaction of the anion with two C−H groups. The global MIPp minimum corresponds to the interaction of the anion with the two C−H groups α to the nitrogen atom with an interaction energy of −75.2 kcal/mol. An additional minimum, which is almost isoenergetic (−74.1 kcal/mol), is found at the opposite part of the map, as a result of the interaction of the anion with H^1 and H^8. The 2D-MIPp(Cl^-) energy map computed at 3.0 Å above the molecular plane predicts the location of the anion over the common C−N bond, to some extent displaced toward the nitrogen atom. These results are in qualitative agreement with the ab initio calculations of complexes **2** and **3**. The main difference resides in the position of the chloride anion, which, in **2c**, is located over the C−N bond and somewhat displaced to the carbon atom and in the MIPp the minimum is displaced to the nitrogen atom.

We have recently demonstrated that the utility of a new tool to predict the geometries of anion--π complexes, where the anion is polyatomic. This tool is entitled the induced-polarization energy map (IPE map). The novelty of this representation is that, in the map, only the contribution of the ion-induced polarization term to the total interaction energy is contoured in a 2D region. The IPE map has been found useful to predict and explain geometries of anion−π complexes of tetrahedral BF_4^- anion with several diazines, triazines, and tetrazines, and it nicely complements the MIPp map.[8b] We have computed the 2D-IPE(F^-) of **1** at 2.8 Å above the molecular plane. The representation is shown in Figure 4 (left, bottom) together with the 2D-MIPp(F^-) (left, top). The corresponding RI-MP2(full)/6−31++G** optimized complexes are also included in Figure 4 (right) to illustrate the agreement of the 2D-IPE/MIPp maps with the geometric features of the complexes. The IPE map indicates that there is a wide region (red contour) that includes both rings where the IPE energy is minimum. We have found two global IPE minima that are represented in the 2D map by red stars. The MIPp minimum is located approximately over the nitrogen atom (represented by a red star in the map). The MP2/6−31++G** optimized complexes $\mathbf{4c_1}$ and $\mathbf{5c_1}$ are in agreement with both maps. The global position of the anion is located where the MIPp map predicts with two fluorine atoms closely located at the lowest isocontour line of the IPE map. Therefore, the 2D-IPE and 2D-MIPp maps can be combined to predict and explain the observed geometric features of the optimized π-complexes. This agreement is most likely observed because the energetically important interactions described by the maps are those used to determine the geometry in the first place when electronic energies are minimized using electron-correlated ab initio methods. In the complexes $\mathbf{4c_1}$ and $\mathbf{5c_1}$, a direct comparison of the MIPp energy values and the MP2/6−31++G** interaction energies is not possible because the MIPp maps are computed using F^- as the interacting particle instead of BF_4^-, because of limitations of the MOPETE-98 program.

C. AIM Analysis. Topological analysis of the charge density ρ(r) distribution and properties of critical points (CP) were determined for complexes **2**−**5** using the Bader's theory of "atoms-in-molecules", which provides an unambiguous definition of chemical bonding,[40] using the MP2(full)/6−31++G** wave function. The AIM theory has been successfully used to characterize anion−π interactions.[5,7] For complexes **2a,b**−**3a,b**, the exploration of the CPs revealed the presence of two bond CPs that connect the anion with two hydrogen atoms. As a consequence of the geometry of the complexes, one ring CP is also generated. In Figure 5, we represent the distribution of CPs that are generated upon complexation of the anion in hydrogen bonding complexes **2a**−**b**, the distribution of CPs in complexes **3a**−**b** is identical, and they are not shown in the figure. For the anion−π complexes **2c**−**3c**, the exploration of the CPs revealed the presence of only one bond CP that connects the anion with the carbon atom of the common C−N bond (see Figure 4, only **2c** is represented). The distribution of CPs in complexes **4**−**5** is more complicated. In hydrogen bonding complexes **4b**−**5b**, the exploration of CPs revealed the presence of four bond CPs and three ring CPs. Two bond CPs connect two fluorine atoms to two hydrogen atoms of the ring, and they properly describe the σ-interaction. The other CPs connect a third fluorine and the boron atoms with three carbon atoms of the ring. This can be considered as a pseudo-π-interaction. The distribution of CPs in the anion−π complexes $\mathbf{4c_{1-2}}$ is very complicated. It can be viewed as a sum of three interactions: First is the interaction of two fluorine atoms of the BF_4^- with both rings of **1**. Each of these two interactions is described by two bond, two ring and one cage CPs. The bond and ring CPs connect the fluorine atom with four carbon atoms of the ring. The cage

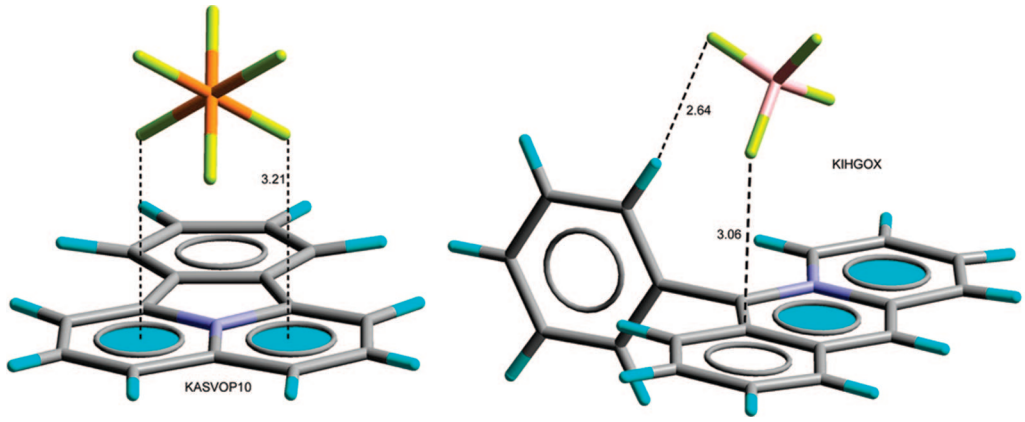

Figure 6. Partial views of the X-ray structures corresponding to **10c**−azoniafluoranthene hexafluorophosphate (KASVOP10, left) and 1-phenylbenzo(**b**)quinolizinium tetrafluoroborate (KIHGOX).

CP connects the fluorine atom with the center of the ring. Second is the interaction of a third fluorine atom of the anion with several atoms of the ring via three bond and two ring CPs in $\mathbf{4c_1}$ and $\mathbf{5c_1}$ and via one bond CP in $\mathbf{4c_2}$ and $\mathbf{5c_2}$. These CPs are located outside the molecular projection in the on-top representation shown in Figure 5. Finally, the third interaction involves the boron atom of the anion, which is connected with **1** through three ring CPs and one cage CP. Quantitative values for $\rho(r)$ and $\nabla^2\rho(r)$ at the CPs give hints on the character and strength of the interaction. These values are summarized in Table 2 for selected CPs that characterize the noncovalent interaction. In all complexes, the value of the Laplacian at the (3, −1) CPs is positive, indicating a depletion of the electron density, as is common in closed-shell interactions. From the data summarized in Table 2, several considerations can be inferred. First, the values of $\rho(r)$ and $\nabla^2\rho(r)$ at the bond CPs in chloride complexes **2a**−**2c** are higher than the ones for bromide complexes **3a**−**3c**, in agreement with the differences in the interaction energies and equilibrium distances. Second, the same is applicable to hydrogen bonding complexes **4b** and **5b** and π-complexes **4c** and **5c**. For latter complexes ($\mathbf{4c_{1-2}}$ and $\mathbf{5c_{1-2}}$), we have used the cage CP because previous studies have demonstrated that the value of the electron charge density at the cage CP can be used as a measure of the bond order in anion−π complexes,[5,7 41] and cation−π interactions.[42] The absolute values of $\rho(r)$ and $\nabla^2\rho(r)$ of anion−π complexes **2c**−**5c** are greater than the ones previously reported in neutral systems like hexafluorobenzene. Moreover, taking into account that the equilibrium distances observed in the anion−π complexes **2c**−**5c** are shorter than the previously reported for standard anion−π complexes, it could be assumed that these complexes contain some degree of covalent character. A more likely explanation is that the interaction of anions with the charged arene **1** involves a strong electrostatic attraction that shortens the equilibrium distances of the complexes. In fact, the values of equilibrium distances and charge density at the CPs present in Tables 1 and 2 are in agreement with the ones obtained for the interaction of anions with the tropylium cation.[23]

D. CSD Analysis. To obtain experimental evidence of the anion-σ/π dual binding affinity of **1**, we performed a search in the Cambridge Structural Database (CSD).[43] Crystal structures are so rich in geometrical information and often reveal effects that have not been noticed by the original authors. The utility of crystallography and the CSD in analyzing geometrical parameters and noncovalent interactions is clearly established.[44] In exploring the CSD for derivatives of quinolizinylium, we have found 23 structures that have been analyzed to determine if the counterion is establishing hydrogen-bonding or anion−π interactions. In Table 3, we summarize the CSD reference codes, the counterion, and the type of noncovalent interaction. It can be observed that spherical anions give in all cases σ interactions, and conversely, they do not participate in anion−π interactions. In contrast, all polyatomic anions participate in anion−π interactions, apart from entry 8. In this structure, the π system is not available for anion−π bonding because it establishes an intermolecular $\pi-\pi$ stacking that controls the crystal packing. The polyatomic anions, in addition to their participation in π-interactions, are also involved in a variety of σ-interactions with other quinolizinylium moieties and a combination of both interactions controls the crystal packing. Two selected examples retrieved from the CSD (codes KASVOP10[45] and KIHGOX[46]) are shown in Figure 6, in which the anion−π interaction is evident and plays a prominent role in the crystal packing. It is remarkable the agreement between the solid state geometry of KASPOV10 and the optimized complex $\mathbf{5c_2}$. In the solid state, the equilibrium distance is larger because the anion is participating simultaneously in a variety of hydrogen bonding interactions with neighboring quinolizinylium moieties.

IV. Concluding Remarks

In summary, we have studied the dual σ/π binding ability of the quinolizinylium cation (**1**), by means of MP2 ab initio calculations, MIPp, and IPE energy maps, and the AIM theory. In addition, we have analyzed the X-ray crystal structures present in the CSD. We have theoretically demonstrated that hydrogen-bonding interactions are more favorable in the complexes of **1** with monatomic anions. In contrast, π-interactions are more favorable in the complexes of **1** with tetrahedral BF_4^- and octahedral PF_6^- anions. These results are in agreement with experimental data obtained from

the CSD. We have demonstrated the utility of MIPp/IPE maps as predictive tools, and we have described the interactions by using the distribution of critical points that emerge upon complexation.

Acknowledgment. We thank the DGICYT of Spain (projects CTQ2005-08989-01 and CTQ2005-08989-02) for financial support. We thank the CESCA for computational facilities. We thank the Govern Balear (project PROGECIB-33A) for financial support.

Supporting Information Available: Cartesian coordinates of RI-MP2/6−31++G** optimized structures **1**−**5**. This material is available free of charge via the Internet at http://pubs.acs.org.

References

(1) Hunter, C. A.; Sanders, J. K. M. *J. Am. Chem. Soc.* **1990**, *112*, 5525.

(2) Meyer, E. A.; Castellano, R. K.; Diederich, F. *Angew. Chem., Int. Ed.* **2003**, *42*, 1210.

(3) Mascal, M.; Armstrong, A.; Bartberger, M. *J. Am. Chem. Soc.* **2002**, *124*, 6274.

(4) Alkorta, I.; Rozas, I.; Elguero, J. *J. Am. Chem. Soc.* **2002**, *124*, 8593.

(5) Quiñonero, D.; Garau, C.; Rotger, C.; Frontera, A.; Ballester, P.; Costa, A.; Deyà, P. M. *Angew. Chem., Int. Ed.* **2002**, *41*, 3389.

(6) Hiraoka, K.; Mizuse, S.; Yamabe, S. *J. Phys. Chem.* **1987**, *91*, 5294.

(7) Schneider, H. J.; Yatsimirski, A. *Principles and Methods in Supramolecular Chemistry*; John Whiley & Sons Ltd: Chichester, U.K., 2000; pp 93−95.

(8) (a) Garau, C.; Frontera, A.; Quiñonero, D.; Ballester, P.; Costa, A.; Deyà, P. M. *ChemPhysChem* **2003**, *4*, 1344. (b) Escudero, D.; Frontera, A.; Quiñonero, D.; Costa, A.; Ballester, P.; Deyà, P. M. *J. Chem. Theory Comput.* **2007**, *36*, 2098.

(9) Demeshko, S.; Dechert, S.; Meyer, F. *J. Am. Chem. Soc.* **2004**, *126*, 4508.

(10) Schottel, B. L.; Bacsa, J.; Dunbar, K. R. *Chem. Commun.* **2005**, 46.

(11) Rosokha, Y. S.; Lindeman, S. V.; Rosokha, S. V.; Kochi, J. K. *Angew. Chem., Int. Ed.* **2004**, *43*, 4650.

(12) de Hoog, P.; Gamez, P.; Mutikainen, I.; Turpeinen, U.; Reedijk, J. *Angew. Chem., Int. Ed.* **2004**, *43*, 5815.

(13) (a) Frontera, A.; Saczewski, F.; Gdaniec, M.; Dziemidowicz-Borys, E.; Kurland, A.; Deyà, P. M.; Quiñonero, D.; Garau, C. *Chem.—Eur. J.* **2005**, *11*, 6560. (b) Gil-Ramirez, G.; Benet-Buchholz, J.; Escudero-Adan, E. C.; Ballester, P. *J. Am. Chem. Soc.* **2007**, *129*, 3820.

(14) García-Raso, A.; Albertí, F. M.; Fiol, J. J.; Tasada, A.; Barceló-Oliver, M.; Molins, E.; Escudero, D.; Frontera, A.; Quiñonero, D.; Deyà, P. M. *Inorg. Chem.* **2007**, *46*, 10724.

(15) Berryman, O. B.; Bryantsev, V. S.; Stay, D. P.; Johnson, D. W.; Hay, B. P. *J. Am. Chem. Soc.* **2007**, *129*, 48.

(16) (a) Gamez, P.; Mooibroek, T. J.; Teat, S. J.; Reedijk, J. *Acc. Chem. Res.* **2007**, *40*, 435. (b) Schottel, B. L.; Chifoides, H. T.; Dunbar, K. R. *Chem. Soc. Rev.* **2008**, *37*, 68. (c) Hay, B. P.; Bryantsev, V. S. *Chem. Commun.* **2008**, 2417.

(17) (a) Tabcharani, J. A.; Chang, X.-B.; Riordan, J. R.; Hanrahan, J. W. *Nature* **1991**, *352*, 628. (b) Quinton, P. M. *Physiol. Rev.* **1999**, *79*, S3.

(18) Welsh, M. J.; Smith, A. E. *Cell* **1993**, *73*, 1251.

(19) Marivingt-Mounir, C.; Norez, C.; Derand, R.; Bulteau-Pignoux, L.; Nguyen-Huy, D.; Viossat, B.; Morgant, G.; Becq, F.; Vierfond, J.-M.; Mettey, Y. *J. Med. Chem.* **2004**, *47*, 962.

(20) Alkorta, I.; Blanco, F.; Elguero, J. *J. Phys. Chem. A* **2008**, *112*, 1817.

(21) (a) Garau, C.; Frontera, A.; Quiñonero, D.; Ballester, P.; Costa, A.; Deyà, P. M. *J. Phys. Chem. A* **2004**, *108*, 9423. (b) Garau, C.; Frontera, A.; Quiñonero, D.; Ballester, P.; Costa, A.; Deyà, P. M. *Chem. Phys. Lett.* **2004**, *392*, 85.

(22) (a) Mascal, M.; Yakovlev, I.; Nikitin, E. B.; Fettinger, J. C. *Angew. Chem., Int. Ed.* **2007**, *46*, 8782. (b) Mascal, M. *Angew. Chem., Int. Ed.* **2006**, *45*, 2890. (c) Berryman, O. B.; Hof, F.; Hynes, M. J.; Johnson, D. W. *Chem. Commun.* **2006**, 506.

(23) Quiñonero, D.; Frontera, A.; Escudero, D.; Ballester, P.; Costa, A.; Deyà, P. M. *ChemPhysChem* **2007**, *8*, 1182.

(24) Ahlrichs, R.; Bär, M.; Hacer, M.; Horn, H.; Kömel, C. *Chem. Phys. Lett.* **1989**, *162*, 165.

(25) Feyereisen, M. W.; Fitzgerald, G.; Komornicki, A. *Chem. Phys. Lett.* **1993**, *208*, 359.

(26) Vahtras, O.; Almlof, J.; Feyereisen, M. W. *Chem. Phys. Lett.* **1993**, *213*, 514.

(27) Frontera, A.; Quiñonero, D.; Garau, C.; Ballester, P.; Costa, A.; Deyà, P. M. *J. Phys. Chem. A* **2005**, *109*, 4632.

(28) Quiñonero, D.; Garau, C.; Frontera, A.; Ballester, P.; Costa, A.; Deyà, P. M. *J. Phys. Chem. A* **2006**, *110*, 5144.

(29) Boys, S. B.; Bernardi, F. *Mol. Phys.* **1970**, *19*, 553.

(30) Luque, F. J.; Orozco, M. *J. Comput. Chem.* **1998**, *19*, 866.

(31) Scrocco, E.; Tomasi, J. *Top. Curr. Chem.* **1973**, *42*, 95.

(32) Francl, M. M. *J. Phys. Chem.* **1985**, *89*, 428.

(33) Luque, F. J.; Orozco, M. *MOPETE-98 Computer Program*; Universitat de Barcelona: Barcelona, Spain, 1998.

(34) (a) Clark, M.; Cramer III, R. D.; Opdenbosch, N. *J. Comput. Chem.* **1989**, *10*, 982. (b) Ujaque, G.; Maseras, F.; Eisenstein, O. *Theor. Chem. Acc.* **1997**, *96*, 146.

(35) (a) Bader, R. F. W. *Chem. Rev.* **1991**, *91*, 893. (b) Bader, R. F. W. *Atoms in Molecules. A Quantum Theory*; Clarendon: Oxford, U.K., 1990.

(36) http://www.AIM 2000.de (accessed Sep 17, 2008).

(37) Sigfridson, E.; Ryde, U. *J. Comput. Chem.* **1998**, *19*, 377.

(38) Mulliken, R. S. *J. Chem. Phys.* **1955**, *23*, 1833.

(39) (a) Emmeluth, C.; Poad, B. L. J.; Thompson, C. D.; Bieske, E. J. *J. Phys. Chem. A* **2007**, *111*, 7322. (b) Thompson, C. D.; Poad, B. L. J.; Emmeluth, C.; Bieske, E. J. *Chem. Phys. Lett.* **2006**, *428*, 18. (c) Loh, Z. M.; Wilson, R. L.; Wild, D. A.; Bieske, E. J.; Zehnacker, A. *J. Chem. Phys.* **2003**, *119*, 9559. (d) Schneider, H.; Vogelhuber, K. M.; Schinle, F.; Weber, J. M. *J. Am. Chem. Soc.* **2007**, *129*, 13022.

(40) Bader, R. F. W. *J. Phys. Chem. A* **1998**, *102*, 7314.

(41) Quiñonero, D.; Garau, C.; Frontera, A.; Ballester, P.; Costa, A.; Deya, P. M. *Chem. Phys. Lett.* **2002**, *359*, 486.

(42) Cubero, E.; Orozco, M.; Luque, F. J. *J. Phys. Chem. A* **1999**, *103*, 315.

(43) Allen, F. H. *Acta Crystallogr.* **2002**, *B58*, 380.

(44) Nangia, A.; Biradha, K.; Desiraju, G. R. *J. Chem. Soc., Perkin Trans.* **2 1996**, 943–953.

(45) Fourmigue, M.; Boubekeur, K.; Batail, P.; Bechgaard, K. *Angew. Chem., Int. Ed. Engl.* **1989**, *28*, 588.

(46) Maassarani, F.; Pfeffer, M.; Le Borgne, G. *Organometallics* **1990**, *9*, 3003.

(47) Elix, J. A.; Sterns, M.; Wilson, W. S.; Warrener, R. N. *J. Chem. Soc. D* **1971**, 426.

(48) Ihmels, H.; Leusser, D.; Pfeiffer, M.; Stalke, D. *J. Org. Chem.* **1999**, *64*, 5715.

(49) Florencio, F.; Smith-Verdier, P.; Garcia-Blanco, S. *Z. Kristallogr.* **1984**, *167*, 29.

(50) Granzhan, A.; Ihmels, H.; Mikhlina, K.; Deiseroth, H.-J.; Mikus, H. *Eur. J. Org. Chem.* **2005**, 4098.

(51) Sato, K.; Arai, S.; Yamagishi, T.; Tanase, T. *Acta Crystallogr., Sect. C: Cryst. Struct. Commun.* **2001**, *57*, 174.

(52) Granzhan, A.; Bats, J. W.; Ihmels, H. *Synthesis* **2006**, 1549.

(53) Ihmels, H.; Mohrschladt, C. J.; Schmitt, A.; Bressanini, M.; Leusser, D.; Stalke, D. *Eur. J. Org. Chem.* **2002**, 2624.

(54) Dai, W.; Petersen, J. L.; Wang, K. K. *J. Org. Chem.* **2005**, *70*, 6647.

(55) Ihmels, H.; Faulhaber, K.; Wissel, K.; Viola, G.; Vedaldi, D. *Org. Biomol. Chem.* **2003**, *1*, 2999.

(56) Yoshino, H.; Koike, K.; Nikaido, T. *Heterocycles* **1999**, *51*, 281.

(57) Sato, K.; Arai, S.; Yamagishi, T.; Tanase, T. *Acta Crystallogr., Sect. C: Cryst. Struct. Commun.* **2003**, *59*, o162.

CT800332Y